SOLAR ELECTRIC PROPULSION GN&C POINTING STATE OVERVIEW FOR THE EMIRATES MISSION TO THE ASTEROID BELT

Riccardo Calaon[*], Cody Allard[†] and Hanspeter Schaub[‡]

The Emirates Mission to the Asteroid Belt (EMA) is an ambitious mission that will heavily leverage Solar Electric Propulsion (SEP) technology. SEP provides efficient thrusting but results in long thrust durations which presents unique GN&C challenges. With the utilization of gimbaling SEP thrusters, the momentum accumulation due to external forces on the spacecraft can be mitigated, while maintaining SEP thrust pointing. Additionally, with the use of articulating solar arrays, the spacecraft can maintain SEP thrust pointing while optimizing power positivity and comply with body fixed keep out zones. This paper outlines the details of the GN&C flight mode with the associated GN&C state has been designed to meet these requirements and is named: the GN&C SEP Pointing State. The requirements, design, and alogrithms are presented with example simulation results showing the applicability and implementation of this GN&C State.

INTRODUCTION

The Emirates Mission to the Asteroid Belt (EMA) is set to launch its explorer in 2028 and will be the first main belt multiple asteroid tour. The explorer will traverse the solar system by using solar electric propulsion (SEP) as the main mechanism for trajectory changes to fly by a total of 7 asteroids, and rendezvous with the seventh. The use of SEP technology enables efficient thrusting resulting in significant mass depletion savings but results in the utilization of the SEP system for long periods of time during the mission. These low thrust missions require creative guidance, navigation and control (GN&C) designs to execute the requirements.

Successful application of electric thrusters in interplanetary missions in history are NASA's Deep Space 1, launched in 1998,[1] JAXA's Hayabusa 1 and 2 missions, launched in 2003 and 2014 respectively,[2,3] ESA's Smart-1 mission, launched in 2003,[4] NASA's Dawn mission, launched in 2007,[5] the ESA-JAXA joint mission Bepi Colombo, launched in 2018[6] and NASA's Psyche mission, launched in late 2023.[7] Of the aforementioned missions, only the Hayabusa missions feature hard-mounted solar arrays whose orientation with the spacecraft hub cannot be changed. Conversely, the other missions feature rotating solar arrays that can be articulated in order to maximize the sunlight incidence and therefore the generated power.[1,4,8] When the desire is to simultaneously align the electric

---

[*]Graduate Research Assistant, Ann and H.J. Smead Department of Aerospace Engineering Sciences, University of Colorado Boulder, Colorado Center For Astrodynamics Research, Boulder, CO, 80303 USA. riccardo.calaon@colorado.edu

[†]Guidance, Navigation and Control Engineer, Laboratory for Atmospheric and Space Physics, University of Colorado Boulder, Boulder, CO, 80303 USA

[‡]Professor and Department Chair, Schaden Leadership Chair, Ann and H.J. Smead Department of Aerospace Engineering Sciences, University of Colorado, Boulder, 431 UCB, Colorado Center for Astrodynamics Research, Boulder, CO, 80309. AAS Fellow, AIAA Fellow.

thruster with the inertial reference and ensure optimal power generation on the arrays, the attitude reference calculation becomes nontrivial due to the presence of multiple, competing pointing constraints. Closed-form solutions for such problem are often scarce in literature. Normally, the focus is put on enforcing the main constraint, i.e. thruster alignment, while the degree of freedom given by the roll about such direction is determined ensuring that the resulting power output satisfies the minimum requirements.

The EMA's MBR Explorer will have two single axis articulating solar arrays, two SEP thrusters, and two two-axis gimbals for controlling the individual SEP thrust directions. Only one SEP thruster will be operated at a time. The GN&C SEP pointing state involves controlling the attitude of the explorer using 4 reaction wheels, articulating the solar arrays towards to the sun to maximize solar power generation, and articulating one the SEP gimbals to acheive the desired inertial thrust direction. These two constraints are enforced via a novel guidance algorithm that computes a closed-form solution for the reference attitude frame that satisfies both the pointing constraints simultaneously. During SEP operations the explorer must manage its angular momentum state due to the reliance on reaction wheels for the attitude control. In addition, the explorer must adhere to keep-out zone pointing constraints and stay within the SEP gimbal articulation limits. A GN&C flight mode with the associated GN&C state has been designed to meet these requirements and is named the "GN&C SEP Pointing State". This paper gives an overview of this pointing state and the full algorithm stack by showing block diagrams, detailed descriptions of algorithms and simulation results.

SEP POINTING REQUIREMENTS AND CONSTRAINTS

The GN&C SEP Point State is created by first considering the requirements during SEP operations. The most relevant requirements are:

1. The spacecraft shall control the SEP DV thrust vector, during SEP operations, to be within 1 deg, 3-sigma, radially about the thrust vector

2. The spacecraft shall control the solar array normals to point towards the Sun to within 5 deg, 3-sigma, during SEP operations

3. The spacecraft shall minimize the angle between the spacecraft body frame +Y axis and the sun direction when completing SEP delta-velocity maneuvers in a commanded inertial direction

4. The spacecraft shall control the build up of momentum such that reaction wheel desaturation is required no more than one time per 7 days

Each of these requirements result in functionality that needs to be incorporated in the GN&C SEP Point Algorithms. Requirement 1 is driven by the mission design and indicates the level of accuracy needed for pointing the SEP thruster. Requirement 2 is driven by power requirements during SEP and ultimately will determine the frequency of updating the solar arrays which is currently set to once every day. Requirement 3 is the keep out zone that is ensuring that the -Y direction of the spacecraft does not see the Sun. Combining requirements 1-3 ultimately lead to the guidance attitude definition during SEP Point. Requirement 4 leads to the necessity to perform autonomous momentum management with the SEP thruster taking advantage of the SEP gimbal's two degrees of freedom.

FUNCTIONALITY FOR SEP POINT STATE

This section discusses the conversion from the requirements in the previous section to functionality and showing block diagrams summarizing this. The functionality that the GN&C SEP Point State must enable is:

1. Nominally point SEP thrust through current spacecraft center of mass (CoM)

2. Maneuver spacecraft to align SEP thrust vector with requested thrust direction

3. Rotate spacecraft about thrust direction to get Solar Array Drive Assembly (SADA) rotation axis (spacecraft X Axis) orthogonal to the Sun and point –Y as far away from the sun as possible

4. Rotate solar arrays to align array normals to the sun direction

5. Autonomous Momentum Management with SEP thruster

   (a) Momentum control authority about axes orthogonal to thrust-CoM line

   (b) Off point both spacecraft and SEP gimbal such that SEP Thruster applies torque about spacecraft CoM that reduces the momentum state of the vehicle (lowering reaction wheel speeds), while also SEP thrust vector aligns with the requested thrust direction.

The ordering of this list does not indicate GN&C algorithm execution order, but the order can be used to build the logic of the guidance algorithms. Each of these items will be focused on in further detail.

Figure 1 is highlighting the logic that is associated with functionality 1, which is aligning the SEP thrust nominally through the CoM of the spacecraft. This is highlighted by the color blue in Figure 1. This is important due to momentum accumulation. If the thrust vector does not go through the CoM of the spacecraft, a torque will be imparted on the spacecraft, and the reaction wheels will have to absorb this momentum. This effectively determines the gimbal orientation in body frame components which will be one aspect of the attitude guidance solution when combined with more information.
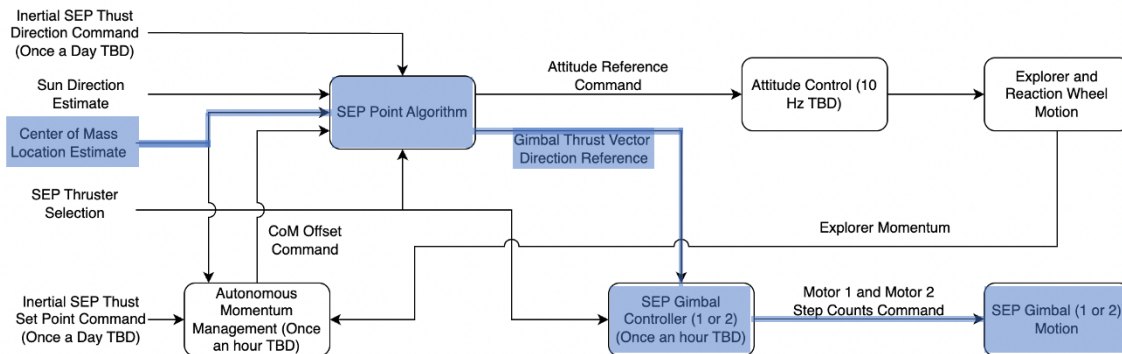

Figure 1: Align Gimbal Through CoM Block Diagram

Now that the thrust vector has been defined in body frame components, Figure 2 shows how that connects with the inertial thrust command. Those two pieces of information lock in two degrees of freedom of the spacecraft because the spacecraft has to align the thrust vector in the body frame, with the requested SEP thrust direction. This completes functionality 2 from above. Another constraint from Figure 2 is the Sun Direction. From functionality 3, the spacecraft will rotate about the thrust vector line to make the SADA axes orthogonal to the sunline. However, this does not completly lock in the attitude of the spacecraft because there are two solutions.[9] The last constraint from functionality 3 is to point -Y as far away from the sun as possible. This removes the ambiguity in the orthogonality condition and fully defines the attitude of the spacecraft.

Functionality 4, rotate solar arrays to align array normals to the sun direction, is not shown on the block diagrams, but is implied functionality for SEP Point.
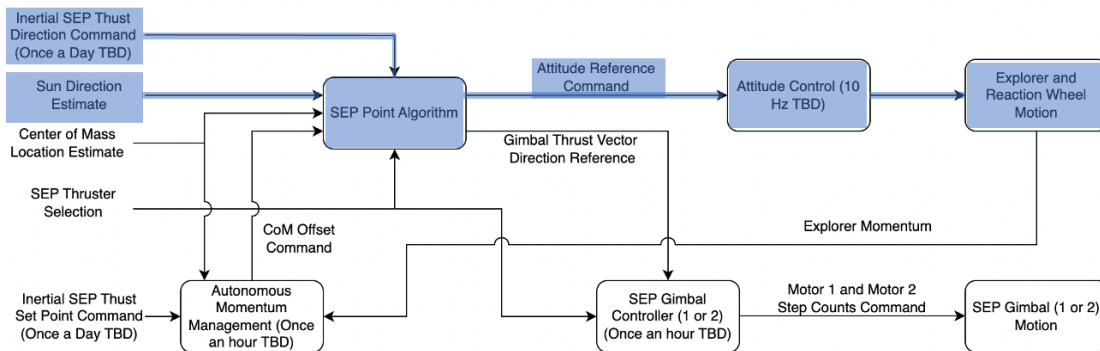

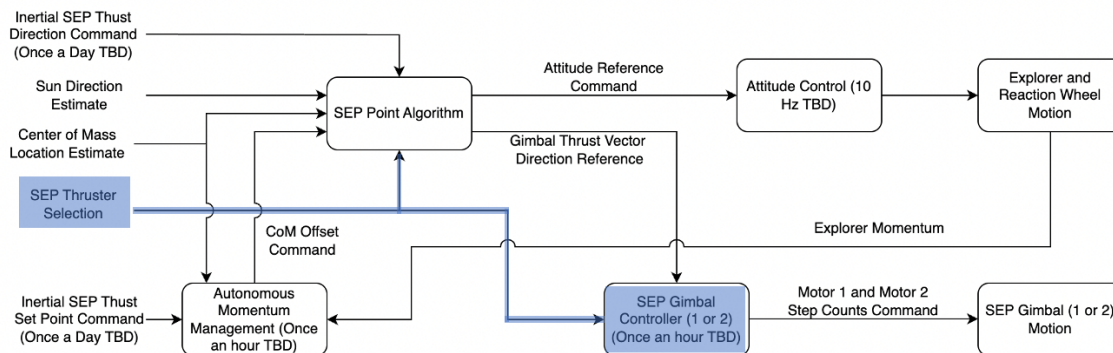**Figure 2**: Define SEP Attitude Block Diagram

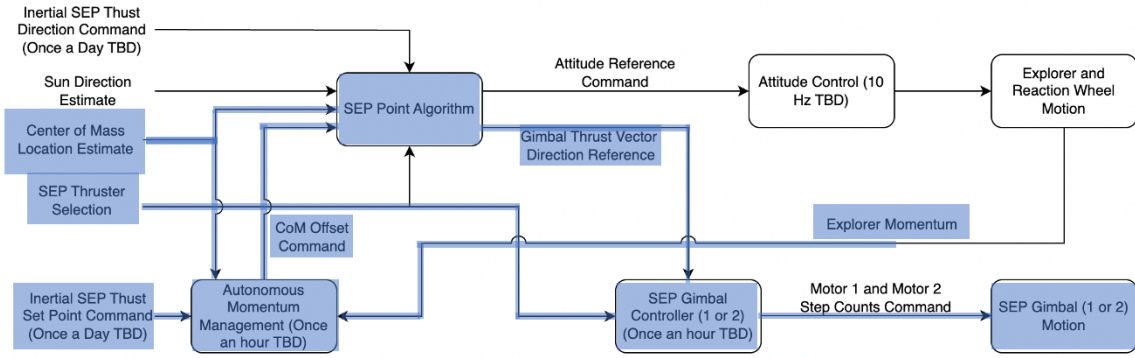**Figure 3**: SEP Thruster Selection Block Diagram

Figure 4: Autonomous Momentum Management with SEP Thruster Block Diagram

Figure 3 is shown here to indicate that for EMA there are two SEP thrusters, and depending on which SEP thruster there will be a different spacecraft attitude and different SEP gimbal controlled.

The last aspect of SEP Point is the autonomous momentum management. This is highlighted in Figure 4. The explorer momentum is fed back to the Autonomous Momentum Management block and returns a CoM Offset Command. Now, instead of the SEP gimbal pointing the thruster through the CoM, there is a commanded off-point with respect to the CoM. This offset is updated every hour to control the momentum build up in the reaction wheels.

Now that the functionality and relationships between the logic of GN&C SEP Point are defined, the algorithms can be detailed further. The follow section outlines the guidance and control algorithms used for SEP Point.

ALGORITHMS OVERVIEW

Guidance

This first subsections describes the guidance algorithms used to provide references for the gimbaled electric thruster, the spacecraft hub attitude, and the solar arrays. As highlighted in the block diagrams, these components are coupled, therefore the guidance algorithms must account for these couplings. The following subsections describe, in order, the guidance algorithms used for each sub-component.

Gimbaled thruster guidance

The thruster dual gimbal can perform tip-and-tild rotations with respect to the body frame. Defining the gimbal frame $\mathcal{F}$, the direction cosine matrix that describes the rotation between $\mathcal{F}$ and $\mathcal{B}$ is described by the tip and tilt angles ν_1 and ν_2:

$$[\mathcal{FB}] = \begin{bmatrix} \cos \nu_2 & \sin \nu_1 \sin \nu_2 & -\cos \nu_1 \sin \nu_2 \\ 0 & \cos \nu_1 & \sin \nu_1 \\ \sin \nu_2 & -\sin \nu_1 \cos \nu_2 & \cos \nu_1 \cos \nu_2 \end{bmatrix} \tag{1}$$

The thrust vector is applied through the origin of the body frame. Point C is the center of mass of the system, and its location is considered known in body-frame coordinates. Let vector $\boldsymbol{c} = \boldsymbol{r}_{C/B}$ denote this quantity.
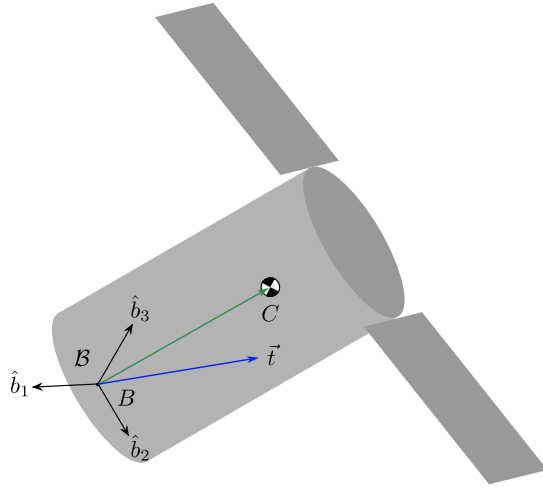
Figure 5: Spacecraft Frame Illustration

The guidance law for the thruster gimbal, however, does not aim to zero the thruster torque acting on the system, but rather to deliver a torque to the spacecraft that counters the momentum buildup due to unmodeled external torques acting on the system. For this reason, the desire is not to align the thruster with the center of mass of the system exactly, but rather with an offset point D located at a distance $\boldsymbol{d}$ from C, as shown in Figure 6. The offset distance $\boldsymbol{d}$ is computed feeding back on the net momentum $\boldsymbol{H}$ on the reaction wheels:

$$\boldsymbol{h} = \sum_{j=1}^{4} I_W \Omega_j \hat{\boldsymbol{u}}_j. \tag{2}$$

with I_W the inertia of the wheels about the respective spin axes, Ω_j the wheel speeds, and $\hat{\boldsymbol{u}}_j$ the unit direction of the spin axes.
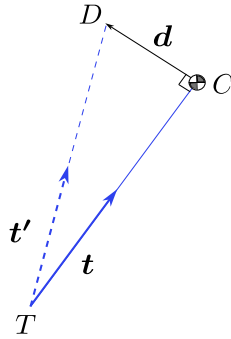

Figure 6: Center of Mass offset

The guidance law that computes the desired offset distance $\boldsymbol{d}$ is:

$$\boldsymbol{d} = -\frac{\boldsymbol{t}}{t^2} \times (\kappa \boldsymbol{h} + \kappa_I \boldsymbol{H}) \tag{3}$$

6

where $\boldsymbol{t}$, according to Figure 6, is the thrust vector when aligned with C. Equation (3) contains the integral of the net wheel momentum:

$$\boldsymbol{H} = \int_0^t \boldsymbol{h}\,\mathrm{d}\tau. \tag{4}$$

This integral term is added to handle uncertainties on the actual center of mass location C, which would cause the momentum to increase over time. The coefficients κ and κ_I are proportional and integral gains, and they have dimensions of Hz and Hz^2, respectively. More details on the derivation of this guidance law can be found in Reference 10.

Attitude guidance

This subsection describes how the attitude reference frame $[\mathcal{RN}]$ is computed. The reference frame is computed as the product of two intermediate frames:

$$[\mathcal{RN}] = [\mathcal{RD}][\mathcal{DN}] \tag{5}$$

where the first intermediate DCM $[\mathcal{DN}]$ ensures that the thrust vector $\boldsymbol{t}$ is aligned with the inertial requested thrust vector $\boldsymbol{t}_{\mathrm{req}}$, whereas the second intermediate DCM $[\mathcal{RD}]$ performs a roll about the thrust vector axis to ensure that the SADA axis $\hat{\boldsymbol{a}}_1$ is orthogonal to the Sun vector $\hat{\boldsymbol{s}}$.

The thrust vector in known in body-frame coordinates from the guidance law in Equation (3), where the thruster is aligned with point D. Knowledge of the instantaneous body-frame $[\mathcal{BN}]$ from attitude measurements allows to express this thrust vector in inertial frame components:

$$^{\mathcal{N}}\hat{\boldsymbol{t}} = [\mathcal{BN}]^T \, {}^{\mathcal{B}}\hat{\boldsymbol{t}}. \tag{6}$$

The principal rotation vector $\hat{\boldsymbol{e}}_\phi$ and principal rotation angle ϕ that describe the first intermediate rotation are immediately found as:

$$^{\mathcal{N}}\hat{\boldsymbol{e}}_\phi = \frac{{}^{\mathcal{N}}\hat{\boldsymbol{t}} \times {}^{\mathcal{N}}\hat{\boldsymbol{t}}_{\mathrm{req}}}{\left|{}^{\mathcal{N}}\hat{\boldsymbol{t}} \times {}^{\mathcal{N}}\hat{\boldsymbol{t}}_{\mathrm{req}}\right|} \qquad\qquad \phi = \arccos\left({}^{\mathcal{N}}\hat{\boldsymbol{t}} \cdot {}^{\mathcal{N}}\hat{\boldsymbol{t}}_{\mathrm{req}}\right), \tag{7}$$

and, from these quantities, the direction cosine matrix $[\mathcal{DN}]$ is readily found. See Reference 11 for a description on how to map principal rotation parameters to DCM.

The second intermediate DCM $[\mathcal{RD}]$ is described by a roll about the thrust vector $\boldsymbol{t}$, by a principal rotation angle ψ. This representation leverages the Gibbs vector, or Classic Rodrigues Parameter set $\boldsymbol{q}$:

$$\boldsymbol{q} = \tan\left(\frac{\psi}{2}\right){}^{\mathcal{B}}\hat{\boldsymbol{t}} = t \cdot {}^{\mathcal{B}}\hat{\boldsymbol{t}}. \tag{8}$$

The expression of the DCM in terms of the CRP set is:[11]

$$[\mathcal{RD}] = \frac{\left((1 - \boldsymbol{q}^T\boldsymbol{q})[\boldsymbol{I}_{3\times3}] + 2\boldsymbol{q}\boldsymbol{q}^T - 2[\tilde{\boldsymbol{q}}]\right)}{1 + \boldsymbol{q}^T\boldsymbol{q}}, \tag{9}$$

however the parameter $t = \tan(\psi/2)$ remains to be determined. The desire is to drive the SADA axis $\hat{\boldsymbol{a}}_1$ orthogonal to the Sun vector $\hat{\boldsymbol{s}}$. This condition is imposed as:

$$^{\mathcal{B}}\hat{\boldsymbol{a}}_1 \cdot [\mathcal{RD}]^{\mathcal{D}}\hat{\boldsymbol{s}} = 0 \tag{10}$$

which can be reformulated into the following equation:

$$\frac{At^2 + Bt + C}{1 + t^2} = 0,$$ (11)

where:

$$A = 2\left(^{\mathcal{D}}\hat{\boldsymbol{s}} \cdot {}^{\mathcal{B}}\hat{\boldsymbol{t}}\right)\left(^{\mathcal{B}}\hat{\boldsymbol{a}}_1 \cdot {}^{\mathcal{B}}\hat{\boldsymbol{t}}\right) - {}^{\mathcal{D}}\hat{\boldsymbol{s}} \cdot {}^{\mathcal{B}}\hat{\boldsymbol{a}}_1$$ (12a)

$$B = 2{}^{\mathcal{B}}\hat{\boldsymbol{a}}_1 \cdot \left(^{\mathcal{D}}\hat{\boldsymbol{s}} \times {}^{\mathcal{B}}\hat{\boldsymbol{t}}\right)$$ (12b)

$$C = {}^{\mathcal{D}}\hat{\boldsymbol{s}} \cdot {}^{\mathcal{B}}\hat{\boldsymbol{a}}_1.$$ (12c)

It can be showed that when the thrust vector is exactly orthogonal to the SADA axis, Equation (11) has two solutions. For this application, the thrust vector is primarily directed along the z body axis, with small deviations from it. Within these bounds, Equation (11) still has two solutions. Solving for t and plugging the result back into Equations (8) and (9) gives the DCM $[\mathcal{RD}]$, which left-multiplied by $[\mathcal{DN}]$ results in the final reference attitude DCM $[\mathcal{RN}]$. More details on the attitude guidance algorithm can be found in Reference 9.

Solar array guidance

Once the reference attitude σ_{RN} is computed, defining the rotation angle for the solar arrays is a relatively trivial problem. The rotation angle of the arrays α_R is defined with respect to a zero direction, for which $\alpha_R = 0$. Such direction $\hat{\boldsymbol{a}}_{2_0}$ is fixed in body-frame coordinates and is, by definition, orthogonal to the SADA axis $\hat{\boldsymbol{a}}_1$. The goal of this section is to identify the reference direction $\hat{\boldsymbol{a}}_{2_R}$ along which to point the surface of the solar arrays. The reference $\hat{\boldsymbol{a}}_{2_R}$ direction is a linear combination of the SADA axis $\hat{\boldsymbol{a}}_1$ and the Sun direction vector $\hat{\boldsymbol{s}}$, and it is orthogonal to the SADA axis:

$$\hat{\boldsymbol{a}}_{2_R} = \frac{\hat{\boldsymbol{s}} - (\hat{\boldsymbol{a}}_1 \cdot \hat{\boldsymbol{s}})\hat{\boldsymbol{a}}_1}{\sqrt{1 - (\hat{\boldsymbol{a}}_1 \cdot \hat{\boldsymbol{s}})^2}}.$$ (13)

The reference angle for the solar arrays is:

$$\alpha_R = \arccos(\hat{\boldsymbol{a}}_{2_R} \cdot \hat{\boldsymbol{a}}_{2_0}).$$ (14)

Control

SEP Gimbal Control

In the present implementation, the SEP Gimbal is actuated via a 2-degree-of-freedom PD controller. The reference gimbal angles ν_{R1} and ν_{R2} are computed by the guidance algorithm. The PD controller acts in order to zero the error between the current gimbal angles and the respective references. Because the gimbal reference angles are updated every hour, the reference gimbal angle rates are always set to zero. The control law takes the form:

$$\boldsymbol{u}_{\mathrm{G}} = -\left[K_{\mathrm{G}}(\nu_1 - \nu_{R1}) + P_{\mathrm{G}}\dot{\nu}_1\right]\hat{\boldsymbol{b}}_1 - \left[K_{\mathrm{G}}(\nu_2 - \nu_{R2}) + P_{\mathrm{G}}\dot{\nu}_2\right]\hat{\boldsymbol{f}}_2.$$ (15)

A future iteration of this work will feature a more faithful model of the SEP Gimbal, which is going to resemble the stepper motor used for the solar array drive assembly.

Attitude Control

The attitude is actuated by means of a nonlinear PID-like control law Modified Rodrigues Parameters (MRPs):[11, 12]

$$
\begin{aligned}
\boldsymbol{u} = &-K\boldsymbol{\sigma}_{\mathcal{B}/\mathcal{R}} - P\boldsymbol{\omega}_{\mathcal{B}/\mathcal{R}} - PK_I\boldsymbol{z} \\
&+ \boldsymbol{\omega}_{\mathcal{B}/\mathcal{N}} \times \left([\boldsymbol{I}_{\text{tot},C}]\boldsymbol{\omega}_{\mathcal{B}/\mathcal{N}} + [\boldsymbol{G}_s]\boldsymbol{h}_s\right) + [\boldsymbol{I}_{\text{tot},C}]\left(\dot{\boldsymbol{\omega}}_{\mathcal{R}/\mathcal{N}} - \boldsymbol{\omega}_{\mathcal{B}/\mathcal{N}} \times \boldsymbol{\omega}_{\mathcal{R}/\mathcal{N}}\right)
\end{aligned}
\tag{16}
$$

where the integral term is defined as:[13]

$$
\boldsymbol{z} = K \int_{t_0}^{t} \boldsymbol{\sigma}_{\mathcal{B}/\mathcal{R}}\text{d}t + [\boldsymbol{I}_{\text{tot},C}]\boldsymbol{\omega}_{\mathcal{B}/\mathcal{R}}.
\tag{17}
$$

The proportional and derivative terms in the control law aim to zero the attitude error and rate error, respectively, between the body frame and the reference frame coming from the guidance algorithm. The scope of the integral term is to counter the effects of unmodeled torques acting on the system. The gyroscopic terms on the second line of Eq. 16 are added to ensure the asymptotic stability of the control law.

Solar Array Drive Assembly Controller

The solar array drive assembly (SADA) controllers are both driving stepper motors. Using the guidance definition defined in previous section of the paper for the solar arrays, the control algorithms commanding the stepper motors are relatively simple algorithms. They take the current position combined with commanded position and the find the necessary steps to achieve the commanded position. Due to this simplicity, SADA controllers are beyond the scope of this paper.

SIMULATION RESULTS

Thruster gimbal performance

This subsection shows the performance of the guidance and control strategies implemented for the gimbaled thruster platform. Figure 7 shows that the desired reference angles for the platform are correctly tracked and the transients only last a couple of minutes. Figure 8 shows the angular offset between the direction of the thrust vector $\boldsymbol{t}$ and the true location of the center of mass with respect to the thrust application point. This offset angle drops as soon as the gimbals are actuated, however in this short simulation this angle settles to around 0.3 deg, with a small thruster offset that counterbalances the action of external unmodeled torques.
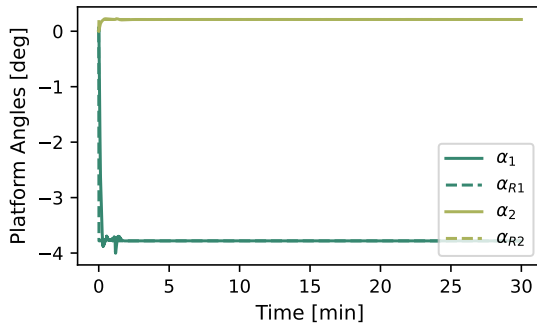

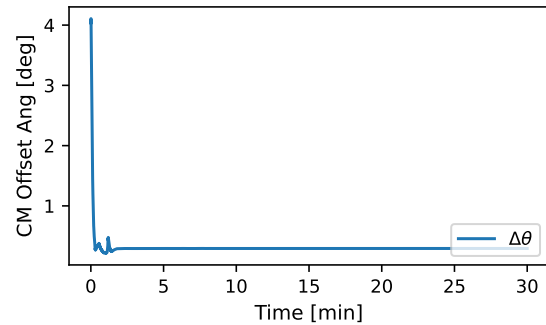**Figure 7**: Thruster gimbal angles and references

Figure 8: Thruster-to-CM offset

Attitude performance

This subsections shows that the attitude guidance and control laws described in the previous section achieve the desired pointing requirements for the spacecraft. Figure 9 shows the MRP attitude error σ_{BR} between the body frame $\mathcal{B}$ and the reference frame $\mathcal{R}$: when the simulation is initiated away from the desired reference frame, the attitude is correctly slewed to reference, ensuring that the attitude error drops to zero with exponential decay. Figure 10 shows the angular error between the thrust vector t and the thrust inertial request t_{req}: it can be seen that, as the spacecraft slews to attitude, this error drops to zero.
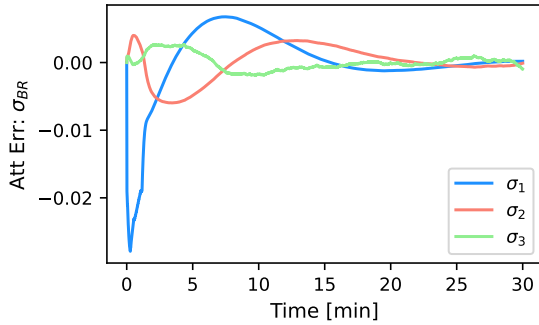

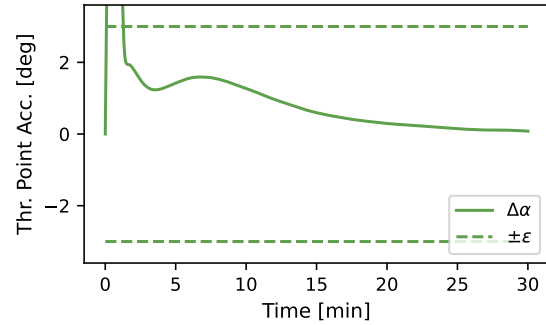**Figure 9**: Attitude tracking error

Figure 10: Thruster pointing performance

Solar arrays performance

The tracking performance of the solar arrays is visualized in Figure 11, where the SADA are actuated by means of stepper motors. The two arrays show symmetric performance as they rotate to track the requested reference angle in order to maximize Sun exposure. Figure 12 shows the angle between the normal to the power-generating surface of the arrays and the sunline: this angle is driven to zero by the combined action of SADA articulation and attitude slew. Figure 12 shows two overlapping plots, as the two arrays behave identically in terms of Sun-tracking performance.
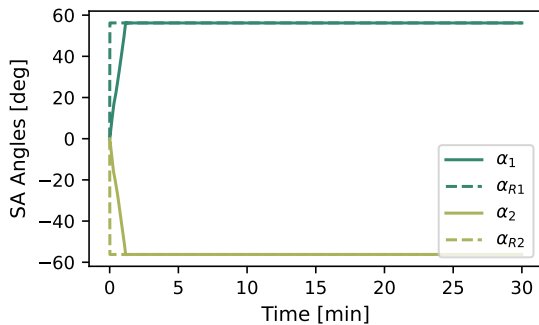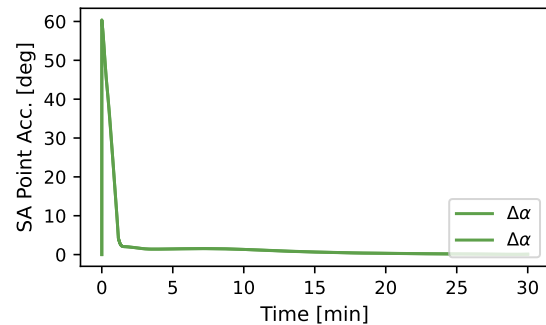

Figure 11: Solar array angles

Figure 12: Solar array pointing performance

Momentum management performance

This section discusses the effectiveness of the guidance law in Equation (3) at managing the momentum buildup on the reaction wheels due to unmodeled external perturbations. This simulation is run for a time window of 7 days, during which the desire is to continuously manage the momentum

10

on the wheels without ever performing desaturation maneuvers using thrusters. For this purpose, the reaction wheels are preemptively biased such that the resulting net momentum is in the opposite direction to the swirl torque exerted by the SEP thruster. Figure 13 shows the reaction wheel speeds over this 7-day window. It is possible to observe some transients at the beginning of the simulation, when the spacecraft is using the reaction wheels to slew to attitude. Past that initial transient, the wheel speeds evolve linearly over time due to a constant swirl torque. Figure 13 shows that the reaction wheels remain within the operational envelope of 75% of the maximum speed allowed.
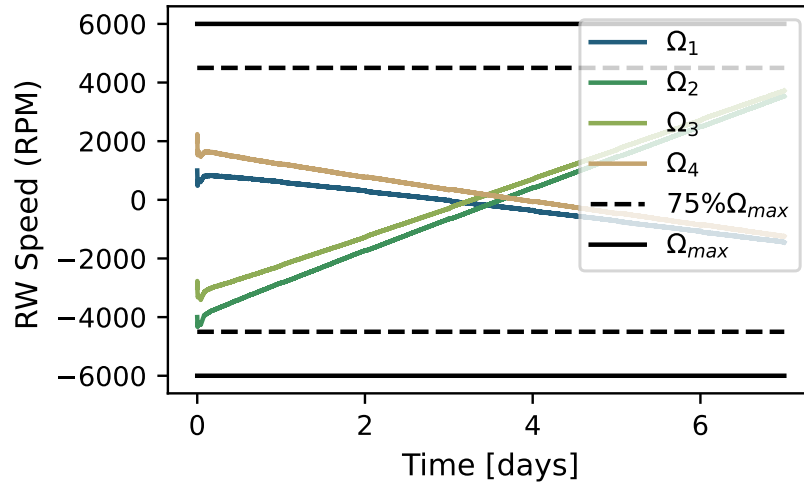

Figure 13: Reaction Wheel speeds

CONCLUSION

The Emirates Mission to the Asteroid Belt (EMA) presents a unique set of challenges for GN&C particularly during periods of Solar Electric Propulsion (SEP) thrusting. This paper outlines the challenges related to pointing constraints and momentum accumulation, the requirements on GN&C to execute SEP sufficiently, and the algorithm and state descriptions for the GN&C flight mode with the associated GN&C state, GN&C SEP Pointing State. Example simulation results are included that show the execution of the GN&C SEP Point State, giving confidence in the implementation. Future work will involve a thorough validation and verification process for the simulation models and flight software algorithms.

ACKNOWLEDGMENTS

REFERENCES

[1] M. D. Rayman and D. H. Lehman, "Deep space one: NASA's first Deep-Space technology validation mission," *Acta Astronautica*, Vol. 41, No. 4-10, 1997, pp. 289–299, 10.1016/s0094-5765(98)00073-3.

[2] M. Yoshikawa, J. Kawaguchi, A. Fujiwara, and A. Tsuchiyama, "The Hayabusa mission," *Sample return missions*, pp. 123–146, Elsevier, 2021, 10.1016/b978-0-12-818330-4.00006-9.

[3] Y. Tsuda, M. Yoshikawa, M. Abe, H. Minamino, and S. Nakazawa, "System design of the Hayabusa 2—Asteroid sample return mission to 1999 JU3," *Acta Astronautica*, Vol. 91, 2013, pp. 356–362, 10.1016/j.actaastro.2013.06.028.

[4] G. Racca, A. Marini, L. Stagnaro, J. Van Dooren, L. Di Napoli, B. Foing, R. Lumb, J. Volp, J. Brinkmann, R. Grünagel, *et al.*, "SMART-1 mission description and development status," *Planetary and space science*, Vol. 50, No. 14-15, 2002, pp. 1323–1337, 10.1016/s0032-0633(02)00123-x.

[5] M. D. Rayman, T. C. Fraschetti, C. A. Raymond, and C. T. Russell, "Dawn: A mission in development for exploration of main belt asteroids Vesta and Ceres," *Acta Astronautica*, Vol. 58, No. 11, 2006, pp. 605–616, 10.1016/j.actaastro.2006.01.014.

[6] A. Loehberg, C. Gruenwald, J. Birkel, A. Brandl, N. Kuebler, H. Perrin, T. Andreev, U. Schuhmacher, and S. Taylor, "The BepiColombo Mercury planetary orbiter (MPO) solar array design, major developments and qualification," *E3S Web of Conferences*, Vol. 16, EDP Sciences, 2017, p. 04006, 10.1051/e3sconf/20171604006.

[7] D. Y. Oh, S. Collins, T. Drain, W. Hart, T. Imken, K. Larson, D. Marsh, D. Muthulingam, J. S. Snyder, D. Trofimov, *et al.*, "Development of the Psyche mission for NASA's Discovery Program," 2019.

[8] B. Heinrich, J. Zemann, and F. Rottmeier, "Development of the BepiColombo MPO Solar Array Drive Assembly (SADA)," *European Space Mechanisms and Tribology Symposium (ESMATS)*, Vol. 87, 2011, pp. 1–21, 10.1016/j.solener.2012.10.005.

[9] R. Calaon, C. Allard, and H. Schaub, "Attitude Reference Generation for Spacecraft with Rotating Solar Arrays and Pointing Constraints," *IEEE Aerospace Conference*, Big Sky, MO, March 2–9 2024. In preparation.

[10] R. Calaon, L. Kiner, C. Allard, and H. Schaub, "Momentum Management Of A Spacecraft Equipped With A Dual-Gimballed Electric Thruster," *AAS Guidance and Control Conference*, Breckenridge, CO, Feb. 2–8 2023. Paper No. AAS-23-178.

[11] H. Schaub and J. L. Junkins, *Analytical Mechanics of Space Systems*. Reston, Virginia: American Institute of Aeronautics and Astronautics, Inc., 4 ed., 2018.

[12] H. Schaub and J. L. Junkins, "Stereographic Orientation Parameters for Attitude Dynamics: A Generalization of the Rodrigues Parameters," *Journal of the Astronautical Sciences*, Vol. 44, No. 1, 1996, pp. 1–19.

[13] S. Krishnan and S. R. Vadali, "An inverse-free technique for attitude control of spacecraft using CMGs," *Acta Astronautica*, Vol. 39, No. 6, 1996, pp. 431–438, 10.1016/s0094-5765(96)00152-x.